02,01

Effect of the microstructure of ultrathin YBaCuO films on the nonlinear microwave response

© E.E. Pestov[1,2], P.A. Yunin[1,2], D.V. Masterov[1], A.E. Parafin[1], S.A. Pavlov[1], E.A. Arkhipova[1], D.A. Savinov[1,2]

[1] Institute for Physics of Microstructures of the Russian Academy of Sciences, GSP-105, Nizhny Novgorod, Russia
[2] Lobachevsky State University, Nizhny Novgorod, Russia

E-mail: pestov@ipmras.ru

Received March 6, 2025
Revised March 6, 2025
Accepted May 5, 2025

Local measurements of the nonlinear microwave response were carried out using the near-field microwave technique for an ultrathin YBaCuO film with an inhomogeneous thickness distribution of 1−6 nm. Its microstructure has been studied using X-ray diffraction analysis. The experimental results indicate that the nonlinear response in the low temperature region may be related to the presence of Andreev bound states in the supercrystalline phase of the YBaCuO film.

Keywords: high-temperature superconductors, near-field microwave microscopy, microstructure, Andreev bound states, ultrathin films.

DOI: 10.61011/PSS.2025.07.61876.12HH-25

1. Introduction

Recently many papers of both applied and fundamental nature have been dedicated to the problem of high-temperature superconductor (HTSC) film microstructure influence at their microwave properties [1]. This interest is primarily caused by the fact that in most experimental situations the observed nonlinear microwave properties of HTSC films depend on both external sources of nonlinearity and fundamental properties of HTSC as such.

One of the fundamental mechanisms of nonlinearity is the nonlinear Meissner effect (NLME) [2,3]. NLME is sensitive to the internal properties of a superconductor, such as the symmetry of the order parameter. In particular, high-temperature superconductors with d symmetry of the gap order parameter can have a strong NLME when the temperature T tends to zero due to low-lying excitations near the nodes of the superconducting gap [4].

At low temperatures the nonlinear microwave response may be attributable to the Andreev bound states (ABS) [5,6], which occur, for example, as a result of the presence of a (110) — oriented surface in high-temperature superconductors. Such interfaces at twin boundaries can be formed spontaneously during the growth of the epitaxial film [7]. Changing the sign of the order parameter results in a strong Andreev reflection of quasiparticles on the surface of the superconductor. A bound state is formed as a result of the interference of electronic and hole excitations, which results in a paramagnetic surface current in a superconductor. The theory [8] predicted a strong temperature dependence of the nonlinearity coefficient equal to $\sim 1/T^3$ at low temperatures for this NLME mechanism. It was also shown that the nonlinear response attributable to ABS can lead to a reversal of the sign of the nonlinear current flowing through the superconductor and a sharp minimum of the temperature dependence of the third harmonic power.

At the same time it was found that due to the small length of HTSC coherence the microstructure of samples impacts the transport and magnetic properties of high quality YBaCuO films. For example, it is known that the critical pinning current of epitaxial films exceeds considerably the critical pinning current of single crystals. Such high value of critical current in YBaCuO films is bound to pinning of vortices at point defects, twin boundaries, precipitates or boundaries of granules (blocks), i.e. with heterogeneity of the structure in high-quality YBaCuO films [9,10].

The strongest impact of the microstructure is observed in the studies of nonlinear microwave properties of HTSC [11–13]. This is related to the fact that nonlinear microwave properties are quite sensitive to various types of defects or intergranular boundaries. In this case Josephson (weak) links are formed between the granules, which result in a nonlinear microwave response in the sample. To describe the microwave response of HTSC block films, a model of chaotic weak links was proposed [14], which described the main features of experimental data at temperatures close to T_c.

The confirmation to the heterogeneity of the YBaCuO film structure are the images obtained using a transmission electron microscope and a scanning tunneling microscope [15,16]. However, it should be noted that these images are usually not used for the studies of the structure correlations with the superconducting properties, since it is not possible to obtain the average structural parameters

of the sample. Therefore, the method of X-ray diffraction analysis is used for the quantitative studies of the HTSC film structure. In this case the width of the X-ray line may be used to determine such structural parameters of the film as the average size of the block (average value of the block coherent scattering region) of epitaxial films, the value of film axis microstrain or disorientation c [17–19].

To study the local nonlinear properties of the high-temperature superconductor films, sensitive near-field microwave microscopes have been developed recently [20–22]. These methods make it possible to conclude on both the microstructure of the sample [23] and on the nature of the superconducting state [21,24].

The temperature dependences of the third harmonic power for the ultrathin YBaCuO film with heterogeneous distribution of $1-6$ nm thickness were studied in this paper using the method of nonlinear near-field microwave microscopy. Using the X-ray diffraction analysis, the rocking curves of the X-ray reflection peak were also studied for this film.

2. Method of study and samples

The nonlinear microwave properties of ultrathin YBaCuO films were studied in this paper using the near-field microwave method [20,24]. This method is based on the registration of a nonlinear microwave response using an inductive type probe. The probe is a thin copper wire with a diameter of 40 μm connecting the inner and outer conductors of the coaxial cable. A high-density alternating current flows in the copper wire since the wave impedance of the coaxial cable is significantly greater than the probe impedance, when the microwave signal is reflected from the near-field probe. This high-frequency current produces a quasistatic magnetic field localized on scales of the order of the probe size. When a strong high-frequency field interacts with the sample under study, higher harmonics of the fundamental frequency arise in the spectrum of the reflected signal because of the nonlinear properties of the superconductor. It should be noted that the near-field probe is used both to generate the microwave field and to record the response of the superconductor to electromagnetic radiation. The frequency of the first harmonic in the experiment was 472 MHz. The level of incident power at the frequency of the first harmonic P_ω ranged from 2 to 10 mW. The local method of nonlinearity study makes it possible to study the spatial distribution of the third harmonic power $P_{3\omega}(x, y)$ of YBaCuO films in the temperature range from 4.2 K to 100 K.

Figure 1 shows the diagram of the near-field microwave probe for scanning along the film (Figure 1). The wire of the probe is parallel to the edge of the film during scanning. The probe is moved mechanically by turning the screw. The scanning step was 0.5 mm. The displacement of the position of the near-field microwave probe is controlled by the angle of rotation of the screw. Its height is set using a 10 μm thick

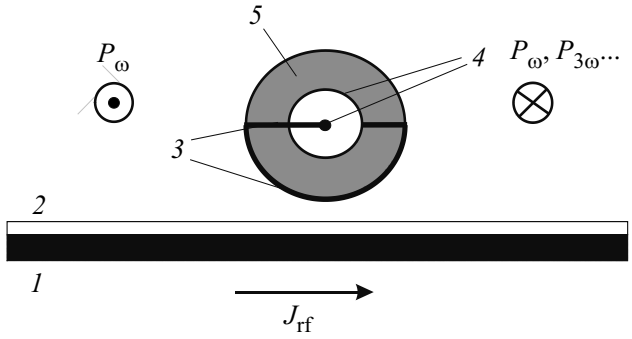

Figure 1. Diagram of a near-field microwave probe for scanning along the film (bottom view): *1* — HTSC film, *2* — Teflon film, *3* — wire of a near-field microwave probe, *4* — coaxial cable, *5* — Teflon coupling. The figure also shows an incident and a reflected microwave signal from the near-field probe and microwave current flowing in the sample.

Teflon film, which is placed between the sample and the near-field microwave probe. The Teflon coupling diameter is 7 mm.

The paper studied the two-layer structure of YBaCuO/Au. An epitaxial YBaCuO film oriented along the axis c, with heterogeneous distribution of $d = 1-6$ nm thickness, was obtained by the method of magnetron sputtering on DC. The film was grown on a $LaAlO_3$ substrate in the form of a disc with a diameter of 32 mm in a gas mixture $Ar(50\,\%)/O_2$ under a pressure of 65 Pa at substrate temperature 840 °C. Under these conditions the estimated deposition rate was around 20 nm/hour. Then a layer of gold with thickness of 20 nm was applied on the YBaCuO film with a minor vacuum gap (*ex situ*), which prevented contact with the surrounding moisture and provided long-term degradation. The golden film was formed by the method of electron beam deposition in high vacuum 10^{-8} Torr at temperature of around 100 °C. Then, using a diamond scriber, the disc was cut into squares with size of 10×10 mm^2 and rectangles with size of 5×10 mm^2 (Figure 2).

The studies of the YBaCuO film microstructure were made by the method of X-ray diffraction analysis using a Bruker D8 Discover diffractometer. The effective thickness of the film was determined using the X-ray diffraction method in the exposure mode of the rocking curve (ω — a scan with a wide gap upstream the detector) by the integral intensity of YBaCuO diffraction reflection (006). The integral intensity of the rocking curve is seemed to be proportionate to the film thickness. The normalizing coefficient is found from the interference measurements of the thickness of test structures with a step. The effective thickness of the film corresponds to the thickness of the homogeneous YBaCuO layer, providing the same integral intensity of diffraction reflection at identical measurement parameters [25]. Besides, the rocking curves of the YBaCuO X-ray reflection peak (006) were measured in different points of the sample (Figure 2).

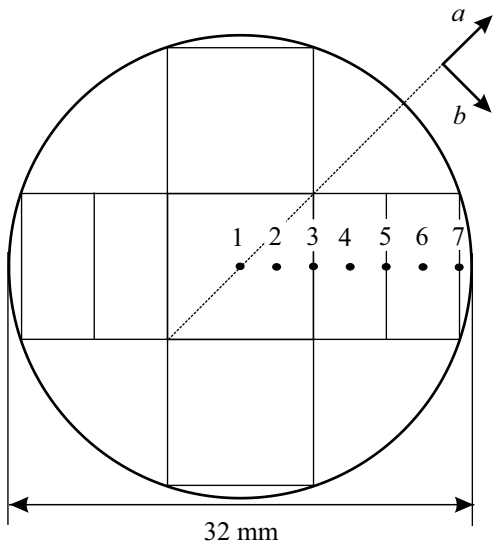

Figure 2. Diagram to make a two-layer YBaCuO/Au structure on a $LaAlO_3$ substrate in the form of a disc. Axes a and b of the YBCO film were rotated by angle 45° relative to the square edges.

3. Experimental results

As it is known, for superconducting YBaCuO films with the thickness of 50–100 nm the temperature dependence of the third harmonic power demonstrates the maximum near the critical transition temperature T_c [20,23]. At the same time, using the method of nonlinear near-field microwave microscopy, the increase of the nonlinear microwave response was recently found in the region of low temperatures for ultrathin YBaCuO films with thickness of 4–5 nm [24,26]. These papers found the dependence of the third harmonic power on the orientation of the wire of the near-field microwave probe in its center. It was found that the maximum value of nonlinearity is observed in the direction of the film axes a–b. The experimental results obtained indicated that the nonlinear microwave response in the low temperature region was associated with the presence of Andreev boundary states occurring at the interfaces of the twin boundaries [24]. It should be noted that thin superconducting films were studied to increase the sensitivity of the experimental setup. This was attributable to the fact that a decrease of their thickness resulted in an increase of the nonlinear microwave signal due to an increase of the density of the superconducting current flowing through it.

At the same time, the question remains why this nonlinearity mechanism was observed in the thickness range of 4–5 nm. Therefore, in this paper we studied the nonlinear microwave response and the microstructure at different thickness of ultrathin YBaCuO films.

Figure 3 shows temperature dependences of the third harmonic power of $P_{3\omega}(T)$ YBaCuO film at various distances R from the disc center. From Figure 3 you can see that the temperature dependence of the nonlinear microwave response demonstrates a maximum near the temperature of the order of 80 K. Besides, an increase of the third harmonic power $P_{3\omega}(T)$ with a decrease of temperature is observed in the low temperature region. As it was shown in paper [24], this increase of the nonlinear microwave response at low temperatures is associated with the presence of the Andreev bound states arising at the interfaces of the twin boundaries.

Figure 4 shows temperature dependences of the third harmonic power of $P_{3\omega}(T)$ YBaCuO film at further increase of the distance R from the disc center. From Figure 4 you can see that with the growth of the distance R the maximum of the third harmonic power $P_{3\omega}(T)$ broadens

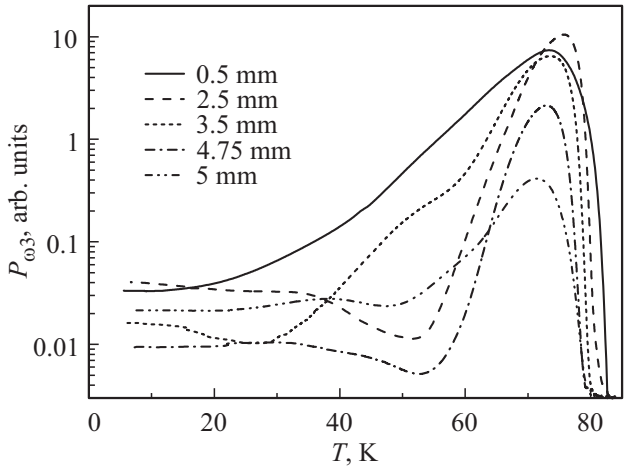

Figure 3. Temperature dependences of the third harmonic power of $P_{3\omega}(T)$ YBaCuO film at various distances R from the disc center. The angle between the direction of the axes a–b and the edge of the sample is 45°. The power of the microwave signal is $P_\omega = 7$ dBm.

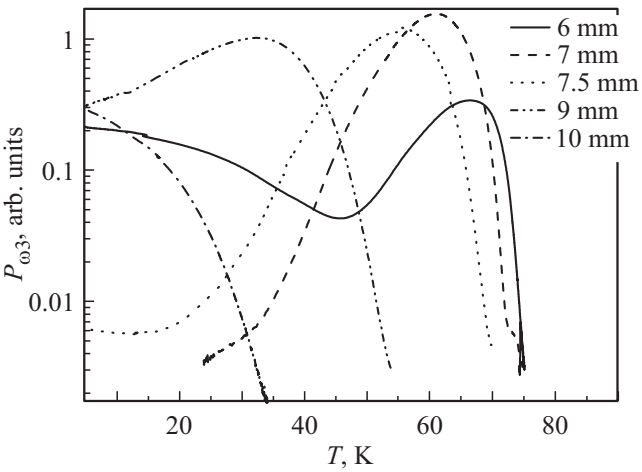

Figure 4. Temperature dependences of the third harmonic power of $P_{3\omega}(T)$ YBaCuO film at various distances R from the disc center. The angle between the direction of the axes a–b and the edge of the sample is 45°. The capacity of the microwave signal is $P_\omega = 3$ dBm.

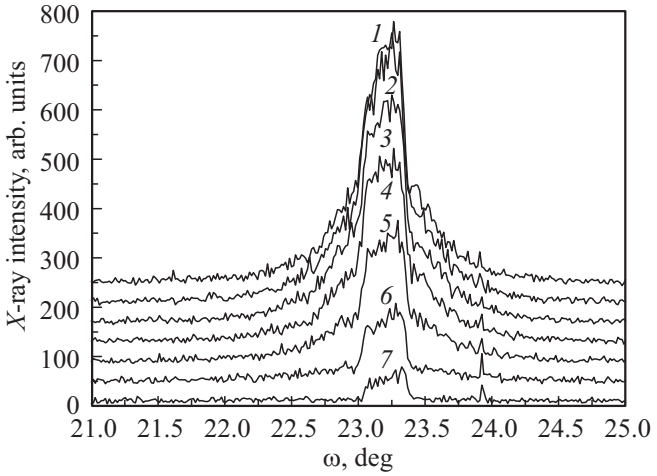

Figure 5. Rocking curves of YBaCuO (006) X-ray reflection peak in different points of the sample. The curves are built with displacement of 40 along the vertical axis.

and shifts towards lower temperatures, which indicates suppression of the critical temperature of the YBaCuO film. It should be noted that at the distance $R = 6$ mm the third harmonic power $P_{3\omega}(T)$ also increases in the low temperature region. It should be noted that in Figure 3 and Figure 4 the microwave signal capacity was chosen for the best observation of low-temperature features at $P_{3\omega}(T)$.

The pattern did not change essentially in scanning with the use of near-field microwave microscopy in the opposite direction of the film. In particular, due to heterogeneity of the superconducting parameters of the YBaCuO film the low-temperature features in the temperature dependence of the third harmonic power were observed at other R values, but at close values of the film thickness.

Figure 5 shows the rocking curves of the YBO (006) X-ray reflection peak in different points of the sample. The table also shows the X-ray data obtained after the processing of the X-ray pictures using the two-peak model. As it is known, the structural perfection of the YBaCuO layer may be characterized by half-width $\Delta\omega$ of the rocking curve, which is associated with the disorientation of the axes from the different mosaic blocks [27,28]. From Figure 5 you can see that the rocking curves have two components. All curves show a narrow peak with half-width of $\Delta\omega_1 = 0.25-0.32$ deg, and as the YBaCuO film thickness increases, these curves show a wider component of $\Delta\omega_2 = 0.82-1.4$ deg. At the same time it should be noted that since the scanning was done using a wide gap, the half-width of the narrow peak of the rocking curve $\Delta\omega$ is also determined by the hardware function of the diffractometer.

It should be noted that since the rocking curves consist of two peaks (Figure 5 and table), it indicates that the film consists of two phases with different orientation of axes c. In the range of thicknesses h_{eff} from 0.5 to 3 nm the film is growing in the form of islands and is a supercrystalline

X-ray data obtained after treatment of X-ray pictures using the two-peak model for a YBaCuO film in different points

№ of point	$I_{\omega 1}$, arb. units.	$\Delta\omega_1$, deg.	$I_{\omega 2}$, arb. units.	$\Delta\omega_2$, deg.	R, mm	h_{eff}, nm
1	40	0.27	105	0.86	0	6
2	42	0.25	110	0.88	2.5	6
3	38	0.27	101	0.82	5	5
4	35	0.29	86	0.94	7.5	4
5	25	0.27	50	1.2	10	3
6	15	0.32	19	1.4	12.5	1.5
7	7	0.27	–	–	15	0.5

phase with minor disorientation of the axis c [29]. In this case the nonlinear microwave response is not observed due to the absence of the continuous flowing of current in the film. At thicknesses above $h_{\text{eff}} = 3$ nm the solid flowing of current occurs in the YBaCuO film, and $P_{3\omega}(T)$ demonstrates a wide peak of nonlinearity at temperature close to T_c (Figure 4). In the range of thicknesses h_{eff} from 3 to 5 nm the temperature dependence $P_{3\omega}(T)$ shows an increase of the nonlinear microwave response at lower temperature (Figure 3 and Figure 4). Therefore, paper [24] showed that firstly, this increase of nonlinearity at low temperatures, secondly, the presence of sharp minimum in $P_{3\omega}(T)$ at temperatures below the critical and, thirdly, the anisotropy of the power of the third harmonic indicate that the nonlinear microwave response in the low temperature region is attributable to the nonlinearity of the Andreev states, arising on the interfaces of the twin boundary. At the same time, since the Andreev edge states are suppressed by disorientation of axis c of the mosaic blocks, we believe that this nonlinearity mechanism is observed in the supercrystalline phase of the YBaCuO film. With further increase of $h_{\text{eff}} > 6$ nm the nonlinear response related to the Andreev edge states is not observed due to stronger disorientation of axis c of the mosaic blocks in the ultrathin YBaCuO film. It should be noted that the broadening of the maximum $P_{3\omega}(T)$ near T_c and suppression of the critical temperature of the YBaCuO film is caused by the decrease in its thickness (Figure 4).

To conclude, it should also be noted that the lateral heterogeneity of the film in thickness is determined by the ratio of the substrate and target erosion area sizes. Under the used operating pressures (dozens of Pa) and the target-substrate distance of more than 30 mm, we find any heterogeneities of the plasma to be without any impact at the lateral heterogeneity of the growing film microstructure. It is directly proven by the fact that as the total thickness of the YBaCuO film increases, the visible differences of the film microstructure in the center and at the edge of the substrate disappear, only the thickness heterogeneity

remains. In this case it is interesting that the only sample makes it possible to most accurately and directly follow the dependence of the YBaCuO microstructure features on the film thickness at the initial stages of growth, i. e. it is not necessary to use the series of various samples obtained in different sputtering cycles.

4. Conclusions

Local nonlinear microwave properties of the YBaCuO ultrathin film with heterogeneous thickness distribution were studied. Using X-ray diffraction analysis and the method of near-field microwave microscopy, it was found that the ultrathin YBaCuO film consists of two superconducting phases with different disorientation of axis c. The experimental results show that the nonlinear microwave response in the low temperature region is caused by the presence of Andreev edge states in the supercrystalline phase of YBaCuO film.

Funding

Equipment provided by the „Physics and Technology of Micro- and Nanostructures“ common use center was used in this study. This study was supported by grant No. 25-22-00204 provided by the Russian Science Foundation.

Conflict of interest

The authors declare that they have no conflict of interest.

References

[1] T.B. Samoilova. Supercond. Sci. Tech. **8**, 259 (1995).
[2] J.C. Amato, W.L. McLean. Phys. Rev. Lett. **37**, 930 (1976).
[3] G.I. Leviev, A.V. Rylyakov, M.R. Trunin. Pisma v ZhETF **50**, 78 (1989). (in Russian).
[4] S.K. Yip, J.A. Sauls. Phys. Rev. Lett. **69**, 2264 (1992).
[5] C.-R. Hu. Phys. Rev. Lett. **72**, 1526 (1994).
[6] Y.S. Barash, M.S. Kalenkov, J. Kurkijärvi. Phys. Rev. B **62**, 6665 (2000).
[7] A.V. Varganov, E.A. Vopilkin, P.P. Vysheslavtsev, Yu.N. Nozdrin, S.A. Pavlov, A.E. Parafin, V.V. Talanov. Pisma v ZhETF **63**, 608 (1996). (in Russian).
[8] A. Zare, T. Dahm, N. Schopohl. Phys. Rev. Lett. **104**, 237001 (2010).
[9] A.A. Polyanskii. A. Gurevich, A.E. Pashitski, N.F. Heinig, R.D. Redwing, J.E. Nordman, D.C. Larbalestier. Phys. Rev. B **53**, 8687 (1996).
[10] J.M. Huijbregtse, B. Dam, R.C.F. van der Geest, F.C. Klaassen. R. Elberse, J.H. Rector, R. Griessen. Phys. Rev. B, **62**, 1338 (2002).
[11] G. Hampel, B. Batlogg, K. Krishana, N.P. Ong, W. Prusseit, H. Kinder, A.C. Anderson. Appl. Phys. Lett. **71**, 3904 (1997).
[12] J. Halbritter. J. of Supercond. **8**, 691 (1995).
[13] P.P. Nguyen, D.E. Oates, G. Dresselhaus, M.S. Dresselhaus. Phys. Rev. B, **48**, 6400 (1993).
[14] T.L. Hylton, A. Kapitulnik, M.R. Beasley. Appl. Rev. Lett. **53**, 1343 (1988).
[15] J. Halbritter. Phys. Rev. B, **48**, 9735 (1993).
[16] Y. Yang, L. Li, Y. Wu. Supercond. Sci. Technol. **10**, 156 (1997).
[17] T.S. Argunova, R.N. Kyutt, M.P. Scheglov, N.N. Faleev. J. Phys. D: Appl. Phys. **28**, A212 (1995).
[18] A.V. Bobyl, M.E. Gaevskii, S.F. Karmanenko, R.N. Kutt, R.A. Suris, I.A. Khrebtov, A.D. Tkachenko, A.I. Morosov. J. Appl. Phys. **82**, 1274 (1997).
[19] D.V. Masterov, S.A. Pavlov, A.E. Parafin, P.A. Yunin. ZhTF **90**, 1677 (2020). (in Russian).
[20] E.E. Pestov, Yu.N. Nozdrin, V.V. Kurin. IEEE Trans. on Appl. Supercond. **11** 131 (2001).
[21] A.P. Zhuravel, B.G. Ghamsari, C. Kurter. Phys. Rev. Lett. **110**, 087002 (2013).
[22] A.P. Zhuravel, S. Bae, S.N. Shevchenko, A.N. Omelyanchouk, A.V. Lukashenko, A.V. Ustinov, S.M. Anlage. Phys. Rev. B **97**, 054504 (2018).
[23] S.V. Baryshev, E.E. Pestov, A.V. Bobyl, Yu.N. Nozdrin, V.V. Kurin. Phys. Rev. B, **76**, 054520 (2007).
[24] E.E. Pestov, M.Yu. Levichev, P.A. Yunin, D.V. Masterov, A.E. Parafin, S.A. Pavlov, D.A. Savinov. FTT **66**, 809 (2024). (in Russian).
[25] B.A. Volodin, A.K. Vorobiev, Yu.N. Drozdov, E.B. Klyuenkov, Yu.N. Nozdrin, A.I. Speransky, V.V. Talanov. Pisma v ZhTF **21**, 90 (1995). (in Russian).
[26] E.A. Arkhipova, A.I. Yelkina, D.V. Masterov, S.A. Pavlov, A.E. Parafin, E.E. Pestov, P.A. Yunin, D.A. Savinov. FTT **66**, 1264 (2024). (in Russian).
[27] R.K. Belov, B.A. Volodin, A.K. Vorobiev, O.P. Vysheslavtsev, S.A. Gusev, Yu.N. Drozdov, E.B. Klyuenkov, Yu.N. Nozdrin, V.V. Talanov. FTT **37**, 785 (1995). (in Russian).
[28] M. Birkholz. Thin Film Analysis by X-Ray Scattering. Wiley–VCH Verlag GmbH & Co. KGaA. (2006). 356 p.
[29] V.F. Solovyov, K. Develos-Bagarinao, D. Nykypanchuk. Phys. Rev. B **80**, 104102 (2009).

Translated by M.Verenikina